Hydrogen Peroxide Photolysis in Acidic Aqueous Solutions Containing Chloride Ions. I. Chemical Mechanism

Xiao-Ying Yu[†,‡] and John R. Barker*[,†,§]

Department of Chemistry, The University of Michigan, Ann Arbor, Michigan 48109-1055, and Department of Atmospheric, Oceanic, and Space Sciences, The University of Michigan, Ann Arbor, Michigan 48109-2143

Received: August 1, 2002; In Final Form: November 19, 2002

Equilibrium constants and rate constants involving $Cl^{\bullet}(aq)$, $Cl_2^{\bullet-}(aq)$, H_2O, and $H_2O_2(aq)$ are measured at 297 ± 2 K by analyzing the kinetics of formation and decay of $Cl_2^{\bullet-}$. The new results are in good agreement with previous studies, when available. The reaction between solvated chlorine atoms and hydrogen peroxide is reported for the first time: $Cl^{\bullet}(aq) + H_2O_2(aq) \rightarrow H^+(aq) + Cl^-(aq) + HO_2^{\bullet}(aq)$, $k_{10} = (2.0 \pm 0.3) \times 10^9$ M^{-1} s^{-1} ($\pm\sigma$). The new results are used along with evaluations of literature data to arrive at recommendations for several key rate constants and equilibrium constants. Of particular interest, the recommended equilibrium constant for the reaction $Cl^{\bullet}(aq) + Cl^-(aq) \leftrightarrow Cl_2^{\bullet-}(aq)$ is $K_5 = (1.4 \pm 0.2) \times 10^5$ M^{-1}($\pm\sigma$).

1. Introduction

Droplets of seawater are released into the air by bursting bubbles in sea foam. The droplets carry organic compounds and minerals (mostly halides), which undergo reactions when exposed to dissolved atmospheric gases and sunlight. Recently, there has been growing interest in atmospheric "halogen activation", by which the relatively unreactive halides are converted to photochemically active halogen compounds.[1−13] Halogen activation has been implicated in the dramatic episodic depletion of ozone in polar regions near the earth's surface (as distinguished from ozone depletion and the ozone holes observed in the stratosphere). The chemical mechanisms that have been proposed to explain tropospheric halogen activation are based on chemical cycles involving oxidation−reduction reactions in the aqueous phase and photolysis reactions in the gas phase. Little attention has been given to possible free radical reactions that may initiate and help to propagate halogen activation. The purpose of the present work is to improve quantitative understanding of aqueous reaction mechanisms and rate constants involving free radicals, so that future modeling studies can assess the contributions made by free radical reactions to atmospheric halogen activation.

In the following, we present a detailed chemical mechanism and measured kinetics parameters for reactions initiated by hydroxyl free radicals in saltwater solutions. The hydroxyl radicals were produced in the laboratory by laser flash photolysis of hydrogen peroxide solutions. In the atmosphere, hydrogen peroxide is ubiquitous, since it is produced by the reactions of hydroperoxyl radicals, which are themselves byproducts of hydrocarbon photooxidation. Because it is highly soluble in water, H_2O_2 dissolves in aqueous aerosols, in clouds, and in rainwater. Photolysis of H_2O_2 is one of the most important sources of aqueous $HO^{\bullet}$ radicals. As in the gas phase, aqueous $HO^{\bullet}$ radicals are highly reactive and attack many species in solution.[14] In sea salt aerosols, almost all $HO^{\bullet}$ radicals react with Cl^-, initiating a rich and chemically complex chain reaction[15−27] that may eventually lead to halogen activation. When some remaining key uncertainties are resolved, it will be possible to assess the contributions of free radicals to tropospheric halogen activation.

Following initiation by $HO^{\bullet}$ radicals in the chloride system, only two reactions are needed to produce the dichloride radical anion ($Cl_2^{\bullet-}$), which remains in pseudo-equilibrium with solvated chlorine atoms (see Table 1). This pseudo-equilibrium is important, because solvated chlorine atoms are far more reactive than $Cl_2^{\bullet-}$. Recent work appears to have settled questions about the magnitude of this equilibrium constant,[16,18,25,27] and the present experiments support those results, leading to only a minor revision in the recommended rate constants. Similar reactions take place in the bromine system.[28] Although the reaction between chlorine atoms and hydrogen peroxide is well-known in the gas phase,[29] it has not been measured previously in solution. In the present work, we report the first measurement of this rate constant.

This paper (paper I) is the first of three papers describing various aspects of the free radical reaction mechanism in chloride solutions. In the second paper[30] (paper II), the $HO^{\bullet}$ radical quantum yield in H_2O_2 photolysis is described using chloride ions as the $HO^{\bullet}$ scavenger. The third paper[31] (paper III) describes the reaction of sulfate radicals with chloride ions and the subsequent mixed first- and second-order decay of $Cl_2^{\bullet-}$ and that of $SO_4^{\bullet-}$ along with new measurements of the optical absorption coefficients for sulfate radicals and $Cl_2^{\bullet-}$ radicals. The effects of ionic strength and temperature on some of the kinetics parameters are also described in paper III. In all of these papers, the same reaction numbering system is used. The recommended rate constants obtained in all three papers are presented with the unified mechanism in Table 1. This is a self-consistent mechanism that gives a good description of the experimental data. In a fourth paper[32] (paper IV), literature data for some important rate constants are critically evaluated.

In the following section, we describe our experimental techniques. We then present the chemical mechanism and a

* To whom correspondence should be addressed. E-mail: jrbarker@umich.edu.

† Department of Chemistry, The University of Michigan.

‡ Present Address: Department of Atmospheric Science, Colorado State University, Fort Collins, CO 80523-1371.

§ Department of Atmospheric, Oceanic, and Space Sciences, The University of Michigan.

10.1021/jp0266648 CCC: $25.00
Published on Web 02/07/2003

TABLE 1: Reaction Mechanism with Recommended Rate Constants, k_i, and Equilibrium Constants, K_i (This Work, Unless Otherwise Noted)

	reaction	k_f	k_r
1	$H_2O_2 + h\nu \rightarrow HO\bullet + HO\bullet$	$\phi_{OH} = 1$[c]	
2	$HO^\bullet + H_2O_2 \rightarrow HO_2^\bullet + H_2O$	$k_2 = (4.2 \pm 0.2) \times 10^7\ M^{-1}\ s^{-1}$ [a]	
3	$HO^\bullet + Cl^- \leftrightarrow ClOH^{\bullet -}$	$k_3 = (4.3 \pm 0.4) \times 10^9\ M^{-1}\ s^{-1}$ [16]	$k_{-3} = (6.1 \pm 0.8) \times 10^9\ M^{-1}\ s^{-1}$ [16]
		$K_3 = 0.70 \pm 0.13\ M^{-1}$ [16]	
4	$ClOH^{\bullet -} + H^+ \leftrightarrow Cl^\bullet + H_2O$	$k_4 = (2.6 \pm 0.6) \times 10^{10}\ M^{-1}\ s^{-1}$ [a]	$k_{-4} = (3.6 \pm 0.4) \times 10^3\ M^{-1}\ s^{-1}$ [a,b]
		$k_4^0 = (3.2 \pm 0.7) \times 10^{10}\ M^{-1}\ s^{-1}$ [a]	
		$K_4 = (7.2 \pm 1.6) \times 10^6$ [a]	
		$K_4^0 = (8.8 \pm 2.2) \times 10^6$ [a]	
5	$Cl^\bullet + Cl^- \leftrightarrow Cl_2^{\bullet -}$	$k_5 = (7.8 \pm 0.8) \times 10^9\ M^{-1}\ s^{-1}$ [b]	$k_{-5} = (5.2 \pm 0.3) \times 10^4\ s^{-1}$ [a]
			$k_{-5} = (5.7 \pm 0.3) \times 10^4\ s^{-1}$ [b]
		$K_5 = (1.4 \pm 0.2) \times 10^5\ M^{-1}$ [a,b]	
6	$Cl_2^{\bullet -} + Cl_2^{\bullet -} \rightarrow 2Cl^- + Cl_2$	$k_6 = (9 \pm 1) \times 10^8\ M^{-1}\ s^{-1}$ [a]	
		$k_6^0 = (7.2 \pm 0.8) \times 10^8\ M^{-1}\ s^{-1}$ [a]	
7	$Cl^\bullet + Cl_2^{\bullet -} \rightarrow Cl^- + Cl_2$	$k_7 = (2.1 \pm 0.05) \times 10^9\ M^{-1}\ s^{-1}$ [d]	
8	$Cl_2^{\bullet -} + H_2O \rightarrow ClOH^{\bullet -} + H^+ + Cl^-$	$k_8[H_2O] < 100\ s^{-1}$ [a]	
9	$Cl_2^{\bullet -} + H_2O_2 \rightarrow HO_2^\bullet + H^+ + 2Cl^-$	$k_9 = (1.4 \pm 0.2) \times 10^6\ M^{-1}\ s^{-1}$ [a]	
10	$Cl^\bullet + H_2O_2 \rightarrow H^+ + Cl^- + HO_2^\bullet$	$k_{10} = (2.0 \pm 0.3) \times 10^9\ M^{-1}\ s^{-1}$ [a]	
11	$Cl_2^{\bullet -} + HO_2^\bullet \rightarrow O_2 + H^+ + 2Cl^-$	$k_{11} = (3.1 \pm 1.5) \times 10^9\ M^{-1}\ s^{-1}$ [e]	
12	$HO_2^\bullet + H_2O_2 \rightarrow H_2O + O_2 + HO^\bullet$	$k_{12} = 0.5\ M^{-1}\ s^{-1}$ [76]	
13	$HO^\bullet + HO^\bullet \rightarrow H_2O_2$	$k_{13} = 6.0 \times 10^9\ M^{-1}\ s^{-1}$ [106]	
14	$HO^\bullet + HO^\bullet \rightarrow H_2O + O^\bullet$		
15	$HO_2^\bullet + HO_2^\bullet \rightarrow H_2O_2 + O_2$	$k_{15} = 9.8 \times 10^5\ M^{-1}\ s^{-1}$ [107]	
16	$HO^\bullet + HO_2^\bullet \rightarrow H_2O + O_2$	$k_{16} = 1.0 \times 10^{10}\ M^{-1}\ s^{-1}$ [108]	

[a] In this paper, uncertainties ($\pm 1\sigma$) were obtained from error propagation; ionic strength (μ) is 0.01 M unless otherwise noted by a superscript "0" on rate or equilibrium constants that have been adjusted to $\mu = 0$. [b] Literature evaluation (this paper), uncertainties ($\pm 1\sigma$) obtained from error propagation. [c] See paper II.[30] [d] See paper III.[31] [e] See paper IV.[32]

discussion of the relevant literature. We go on to explain how we tested the accuracy of the mechanism and carried out measurements of rate and equilibrium constants. The results are presented and discussed in relation to the literature.

2. Experimental Section

The experimental apparatus is similar in many ways to that used in previous work,[33,34] and a detailed discussion of the experimental techniques can be found in paper II[30] and in a Ph.D. dissertation.[35] Briefly, a pulsed rare gas−halogen excimer laser was used to photolyze hydrogen peroxide at 297 ± 2 K. A high-pressure xenon−mercury arc lamp provided a continuous light source for monitoring transient species by absorption. Dichloride radical anion ($Cl_2^{\bullet -}$) was monitored by its absorption at 364 nm ($\epsilon(Cl_2^{\bullet -}, 364\ nm) = 7000 \pm 700\ M^{-1}\ cm^{-1}$, base 10),[31] which is the wavelength of the strongest output band of the xenon−mercury lamp in the vicinity of the $Cl_2^{\bullet -}$ absorption maximum (~340 nm). This value for the extinction coefficient of $Cl_2^{\bullet -}$ was determined[31] by the photolysis of solutions containing $SO_4^{\bullet -}$ and Cl^- using the same experimental setup as described here (see paper III for details). The basic approach was to compare the absorptions due to $SO_4^{\bullet -}$ and to $Cl_2^{\bullet -}$, where the extinction coefficient employed for $SO_4^{\bullet -}$ was the same as that measured recently by Buxton et al.[36] The resulting extinction coefficient for $Cl_2^{\bullet -}$ (given above) is within 15% of most of the previous values at the wavelength of maximum absorption (see paper III for details and for an error analysis).

Under the experimental conditions, the concentration of solvated $Cl^\bullet$ atoms was very small and their light absorption ($\epsilon(Cl^\bullet, 364\ nm) \approx 2000\ M^{-1}\ cm^{-1}$, base 10)[37] could be neglected as compared to that of $Cl_2^{\bullet -}$. White cell optics were utilized to fold the optical path in the cell in order to enhance detection sensitivity.[38] A monochromator equipped with a photomultiplier was used to monitor the transmitted light. The output was amplified and sent to a digital oscilloscope and computer for signal averaging and analysis. Least-squares fits of the experimental data were carried out using KaleidaGraph[39] software,

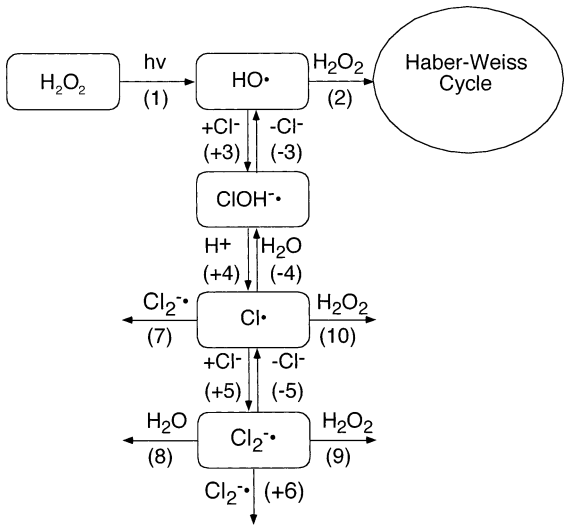

Figure 1. Schematic diagram of the reaction mechanism. Numbers in parentheses correspond to reaction numbers in Table 1.

which utilizes the Levenberg−Marquardt nonlinear least-squares algorithm.[40] When weighted data analysis was performed, weighting was based on the error of each of the data points. Some typical time profiles of the absorption of $Cl_2^{\bullet -}$ with nonlinear least-squares fits are shown in Figure 2.

All solutions were prepared immediately before the experiments. The water was purified by a Milli-RO/Milli-Q system (the water resistivity was ≥18 MΩ cm). All reagents were of ACS grade. Sodium chloride (99.999%) and anhydrous sodium perchlorate (98−102%) were purchased from Alfa ÆSR. Perchloric acid ($HClO_4$, 70%) was purchased from Aldrich. Potassium persulfate ($K_2S_2O_8$, ≥99.0%) and hydrogen peroxide (inhibitor-free H_2O_2, 30%) were obtained from Fisher Scientific. Hydrogen peroxide was assayed daily in the laboratory by the iodine method.[41] The concentration of H_2O_2 utilized in the experiments was usually $\sim 10^{-4}$ M for photolysis at 248 nm and $\sim 10^{-2}$ M for photolysis at 308 nm. No other electrolyte

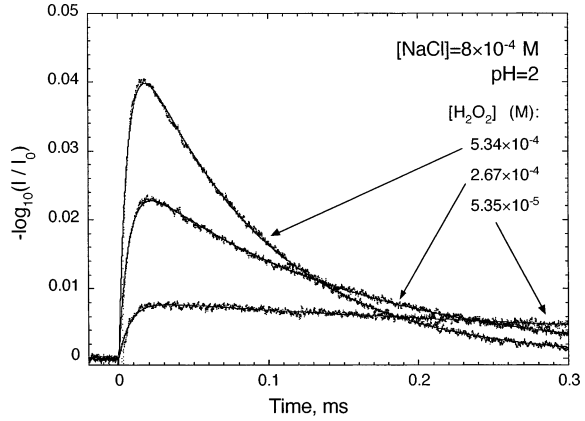

Figure 2. Typical time profiles of the rise and decay of $Cl_2^{\bullet-}$ when [NaCl] is $< 1 \times 10^{-3}$ M. The solid lines are nonlinear least-squares fits (unweighted). Experimental conditions: pH = 2, [NaCl] = 8×10^{-4} M.

was added to the solution to adjust the ionic strength of the solution. The pH (0−4) of all of the solutions was controlled by adding perchloric acid ($HClO_4$) and measured with a Digital Ionalyzer (Orion Research 501) calibrated with appropriate pH buffer solutions (Fisher).

All experiments were carried out at room temperature (297 ± 2 K). The solutions contained dissolved air, unless specifically mentioned otherwise. In some experiments, the dissolved air was purged by bubbling with argon gas (99.999%) from Liquid Carbonic Corporation. It was found that dissolved air does not affect the kinetics of the system.

3. Chemical Mechanism

Various approaches have been used to study the kinetics of $Cl_2^{\bullet-}$ in the past. Many investigations have been carried out by using pulse radiolysis or flash photolysis of persulfate ions ($S_2O_8^{2-}$) in a chemical system containing chloride ions.[15,17,19−26,42−50] The photodissociation of persulfate ions generates sulfate radicals ($SO_4^{\bullet-}$), which react with Cl^- and produce $Cl_2^{\bullet-}$ after two reaction steps. On the basis of this prior work and on the present work (described below), we arrived at the chemical mechanism in Table 1.

3.1. Formation and Decay of $Cl_2^{\bullet-}$. The overall reaction of $HO^\bullet$ with Cl^- to produce $Cl_2^{\bullet-}$ was discovered to be pH-dependent in several investigations.[42,51,52] Reactions 3 and 4 were first proposed by Anbar and Thomas,[42] who assumed that reaction 3 has a diffusion-controlled rate constant of 2×10^{10} M^{-1} s^{-1}. Although they attempted to verify the existence of $ClOH^{\bullet-}$ by measuring the effect of chloride ions (up to 10 mM) on the reaction rate and by detecting $HO^\bullet$ radical through its reactions with benzene and ferrocyanide, they could not achieve confirmation. Furthermore, no appreciable D_2O isotope effect was observed, contrary to expectations based on reaction −4. Anbar and Thomas concluded that further work was needed to confirm the reaction mechanism.

In 1973, Jayson et al.[16] observed the spectrum of $ClOH^{\bullet-}$ in the pulse radiolysis of solutions that contained dissolved N_2O and concentrated chloride at neutral pH. They confirmed that $ClOH^{\bullet-}$ reacts with H^+ to yield $Cl^\bullet$ and that $Cl_2^{\bullet-}$ is formed in the subsequent reaction of $Cl^\bullet$ with Cl^-. Jayson et al. also measured forward and reverse rate constants for reactions 3−5 under acidic conditions and confirmed that those reactions are important for $Cl_2^{\bullet-}$ formation. Nagarajan and Fessenden[53] showed that after $Cl_2^{\bullet-}$ is temporarily depleted by pulsed laser photolysis, its rate of recovery depends on $[H^+]$, thus confirming the role of reaction 4. On the basis of the findings by Anbar and Thomas,[42] Jayson et al.,[16] McElroy,[48] and Buxton et al. proposed that an intermediate species, $HOClH^\bullet$, is produced by reaction of $ClOH^{\bullet-}$ with H^+. The transient existence of $HOClH^\bullet$ is possible, but the present experiments provide no indications of its existence, probably because it dissociates into $Cl^\bullet + H_2O$ on a very short time scale. Because it is not a factor in the present experiments, it has been neglected in writing reactions 4 and −4.

The equilibrium constant for reaction 5 (K_5; equilibrium constants for a reaction *i* are denoted in this paper by an upper case "K_i") has been the subject of several investigations. Literature values for K_5 near 20 °C are scattered over about 4 orders of magnitude,[16,18,25,27] although the recent value obtained by Buxton et al.[25] agrees reasonably well with that of Jayson et al.[16] One of the objectives of the present work was to determine K_5 independently. As described below, we have measured the rate constant (k_{-5}) of the reverse reaction and then combined this value with a literature value of k_5 (for the forward reaction) to obtain the equilibrium constant K_5. The result is shown below to be in good agreement with Jayson et al.[16] and Buxton et al.[25] but has reduced uncertainty.

The decay of $Cl_2^{\bullet-}$ has been investigated in great detail by both pulse radiolysis and flash photolysis. At very low $Cl_2^{\bullet-}$ concentrations, the observed decay follows first-order kinetics and at high $Cl_2^{\bullet-}$ concentrations it follows second-order kinetics. In general, the observed decay is best described using mixed first-order and second-order kinetics.[48,49] The second-order $Cl_2^{\bullet-}$ decay due to reaction 6 has been investigated by many workers,[18,19,44,46−48,54−65] but the measured rate constants show very large discrepancies. At high chloride concentrations and when the concentration of $Cl_2^{\bullet-}$ is high, the principle second-order reaction is reaction 6, between two $Cl_2^{\bullet-}$ radicals. At low chloride concentrations, solvated chlorine atoms in equilibrium with $Cl_2^{\bullet-}$ (via reaction 5) contribute significantly to the second-order decay by reacting with $Cl_2^{\bullet-}$ according to reaction 7.[31] When $HO_2^\bullet$ radicals are present in concentrations similar to that of $Cl_2^{\bullet-}$, reaction 11 contributes another second-order component to the $Cl_2^{\bullet-}$ decay.[46,61,66] In summary, reactions 6, 7, and 11 can contribute to the second-order decay of $Cl_2^{\bullet-}$ under various conditions.

The pseudo-first-order decay of $Cl_2^{\bullet-}$ is due to reactions involving $Cl_2^{\bullet-}$, itself, as well as to reactions involving solvated Cl atoms, since the Cl atoms are usually in near-equilibrium with $Cl_2^{\bullet-}$ according to reaction 5. The well-known reaction −4 of $Cl^\bullet$ with H_2O contributes to the pseudo-first-order decay of $Cl_2^{\bullet-}$.[16,25,45,48] The reaction of $Cl_2^{\bullet-}$ and H_2O has also been postulated, although its rate is slow and quite uncertain.[25,47−49] There have been several reports of reaction 9 between $Cl_2^{\bullet-}$ and H_2O_2.[67−69] Reaction 9 is reported to have a larger rate constant than that of reaction 8 between $Cl_2^{\bullet-}$ and H_2O, but there are large discrepancies among the reported rate constants. In the gas phase, reaction 10 between $Cl^\bullet$ and H_2O_2 has a large rate constant,[29] but it has not been reported in the aqueous phase. One of our objectives was to measure the rate constant for reaction 10, and our results are described below. In summary, reactions −4 and 8−10 contribute to the pseudo-first-order decay of $Cl_2^{\bullet-}$ under various experimental conditions utilized in the present experiments.

3.2. Haber−Weiss Cycle. Under acid conditions, the free radical chain carriers in the decomposition of hydrogen peroxide are $HO^\bullet$ and $HO_2^\bullet$ free radicals.[70] In the absence of chloride ions, the free radical chain mechanism (the Haber−Weiss mechanism) consists of reactions 2 and 12−16.[71−78] Reaction

14 has never been reported in the aqueous phase, although it is known in the gas phase; it is included in Table 1 for completeness. When the chloride ion concentration is low, the $HO^{\bullet}$ radicals can attack H_2O_2 and initiate the Haber−Weiss mechanism. Under most of the experimental conditions utilized in the present work, only reaction 2 is important, but the full Haber−Weiss mechanism is included in Table 1 for completeness.

4. Data Analysis

4.1. Strategy. The mechanism shown in Table 1 and Figure 1 is complicated, but it simplifies considerably under certain experimental conditions. This is because the rate-limiting steps to a large extent can be selected by controlling the $[Cl^-]$, $[H_2O_2]$, and pH. For example, if the pH is very low, then reaction 4 is very fast and by controlling $[Cl^-]$ the rate-limiting steps along the path to the formation of $Cl_2^{\bullet-}$ will be either reaction 3 or reaction 5. By controlling the $[Cl^-]/[H_2O_2]$ ratio, reaction 2 of $HO^{\bullet}$ with H_2O_2 can be made to compete with reactions 3 and 5. If $[Cl^-]$ is large, then reactions 3 and 5 will be very fast, and the rate-limiting step will be reaction 4, which depends on pH. Although many reactions are listed in Table 1, the most important ones are reactions 2, ±3, ±4, ±5, and 6. In the following analysis, we obtain values for rate constants and/or equilibrium constants for most of these reactions under conditions that minimize interferences and correlations in the least-squares analysis.

We did not apply any estimated adjustments for ionic strength in the present analysis because the ionic strength was nearly constant (∼0.01 M) in all of the experiments and only reactions 4 and 6 were affected. Moreover, the estimated effects are relatively small (∼20%), as described in section 5.1.

As described above, $Cl_2^{\bullet-}$ is expected to follow mixed first- and second-order kinetics.[16,25,45,48,49,67] However, at low radical concentrations, the second-order contributions become insignificant. At low $[Cl^-]$ ($<10^{-3}$ M) and low free radical concentrations ($\leq 10^{-6}$ M), the mechanism can be approximated by neglecting the second-order reactions. The accuracy of this approximation was tested by carrying out a mixed first- and second-order least-squares analysis for many of the experiments. We found that the relative uncertainties in the second-order parameters deduced in this way were large and the first-order parameters determined in this way were not significantly affected by neglecting the second-order contributions. Hence, the second-order reactions are neglected in most of the following analysis.

The appearance of the $Cl_2^{\bullet-}$ absorption signals varies significantly when the initial concentration of chloride ion varies. Typical time profiles of the rise and decay of $Cl_2^{\bullet-}$ when $[Cl^-]$ is less than 1×10^{-3} M are shown in Figure 2. The solid lines show the nonlinear least-squares fits according to eq I and Beer's law. The rising portion of a time profile corresponds to the faster pseudo-first-order rate constant (k_A or k_B), and the falling portion corresponds to the slower step.

An analytical expression for $[Cl_2^{\bullet-}]$ can be derived from the chemical mechanism by (i) neglecting reactions that are second order in free radical concentrations and (ii) making the quasi-steady state approximation for Cl atoms and for $ClOH^{\bullet-}$: The analytical expression for $[Cl_2^{\bullet-}]$ is derived in the Appendix and given by eq I:

$$[Cl_2^{\bullet-}] = C[HO^{\bullet}]_o\{e^{-k_A t} - e^{-k_B t}\} \quad \text{(I)}$$

where the proportionality constant C is defined in the Appendix

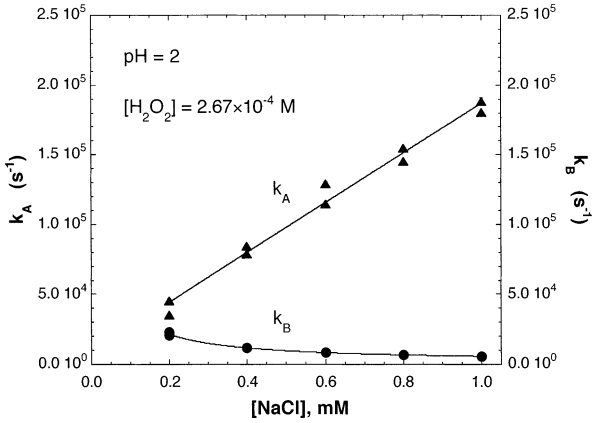

Figure 3. Plot of k_A (triangles) and k_B (circles) vs [NaCl]. The $\pm 1\sigma$ statistical errors are about the same size as the data points. The solid lines are unweighted least-squares fits. Experimental conditions: pH = 2, $[H_2O_2] = 2.67 \times 10^{-4}$ M.

and

$$k_A = k_2[H_2O_2] + k_g[Cl^-] \quad \text{(IIa)}$$

$$k_g = \frac{k_3 k_4[H^+]}{k_{-3} + k_4[H^+]} \quad \text{(IIb)}$$

$$k_{-g} = \frac{k_{-3}k_{-4}[H_2O]}{k_{-3} + k_4[H^+]} \quad \text{(IIc)}$$

$$k_B = \{(k_8^I + k_9[H_2O_2])k_5[Cl^-] + (k_{-g}[H_2O] + k_{10}[H_2O_2])(k_{-5} + k_8^I + k_9[H_2O_2])\}\Big/\{k_5[Cl^-] + k_{-5} + k_{-g}[H_2O] + k_{10}[H_2O_2] + k_8^I + k_9[H_2O_2]\} \quad \text{(III)}$$

where $k_8^I = k_8[H_2O]$. Under the acidic conditions used in this work (see below), the expressions for k_g and k_{-g} become simpler because $k_{-3} \gg k_4[H^+]$; hence, $k_g \approx K_3 k_4[H^+]$ and $k_{-g} \approx k_{-4}$. When $[H_2O_2]$ is low enough, the rates of reactions 5 and −5 dominate the formation and the loss, respectively, of $Cl_2^{\bullet-}$, and eq III is greatly simplified:

$$k_B = \left\{\frac{k_8 K_5[Cl^-] + k_{-g}}{K_5[Cl^-] + 1}\right\}[H_2O] + \left\{\frac{k_9 K_5[Cl^-] + k_{10}}{K_5[Cl^-] + 1}\right\}[H_2O_2] \quad \text{(IVa)}$$

or

$$k_B = I + S[H_2O_2] \quad \text{(IVb)}$$

Equation IV is very useful in the analysis of the experimental data.

Rate constants k_A and k_B are functions of both H_2O_2 and $[Cl^-]$. Data such as those shown in Figure 3 were fitted to eq I in order to find rate constants k_A and k_B. Representative results for constant pH and $[H_2O_2]$ are shown in Figure 3 as a function of $[Cl^-]$. From the least-squares fit of a single experiment, it is only possible to find two fitted rate constants, but it is not possible to identify which rate constant corresponds to k_A and which one to k_B. However, by carrying out experiments over a range of $[Cl^-]$ (see eqs IIa and III), it is possible to identify the rate constants: the rate constant that is linearly proportional to $[Cl^-]$ is identified with k_A (eq IIa) and the other is identified

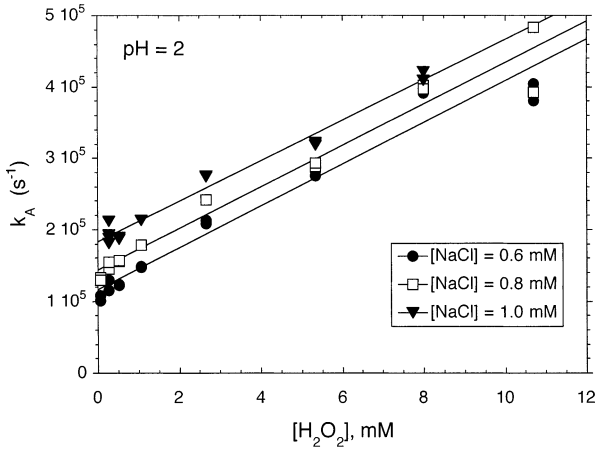

Figure 4. k_A vs $[H_2O_2]$ at various [NaCl] and pH = 2. The solid lines are unweighted linear least-squares fits. The $\pm 1\sigma$ statistical errors are about the same size as the data points.

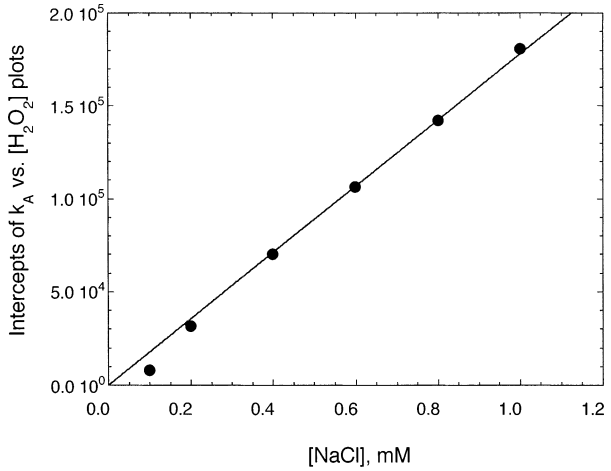

Figure 5. Plot of intercepts (from unweighted linear least-squares fits of k_A vs $[H_2O_2]$) vs [NaCl]. The solid line is an unweighted linear least-squares fit constrained to pass through the origin. The $\pm 1\sigma$ statistical errors are about the same size as the data points.

TABLE 2: Results from k_A Analysis at 297 ± 2 K with Statistical Precision ($\pm 1\sigma$)

eq II	directly measured results
from intercepts	$k_4K_3 = (1.80 \pm 0.03) \times 10^{10}\ M^{-1}\,s^{-1}$
from slopes	$k_2 = (4.2 \pm 0.2) \times 10^{7}\ M^{-1}\,s^{-1}$

with k_B (eq IV). This identification is unambiguous, as is apparent from the data shown in Figure 3.

4.2. Analysis Based on k_A. Fitted rate constant k_A in eq II depends on rate constants k_2 and k_g. According to eq IIb, $k_g \approx K_3k_4[H^+]$ when $k_{-3} \gg k_4[H^+]$. At pH = 2, this condition is achieved, as discussed below. Thus, the analysis of k_A at pH = 2 can give information about k_2 and K_3k_4. The kinetic information obtained from the k_A analysis is listed in Table 2.

A plot of k_A vs $[H_2O_2]$ at various chloride concentrations and pH = 2 is shown in Figure 4 (in the interest of clarity, only some of the data are shown). The value of $k_2 = (4.2 \pm 0.2) \times 10^7\ M^{-1}\ s^{-1}$ is obtained directly from the slopes of the linear least-squares fits. Our result is consistent with previous measurements obtained by both direct methods[78−80] and competition methods.[71,81−88]

The intercepts of the lines in Figure 4 are equal to the product $k_g[Cl^-]$ and are shown in Figure 5 as a function of chloride concentration. The slope of the line in Figure 5 is the rate constant $k_g = (1.80 \pm 0.03) \times 10^8\ M^{-1}\ s^{-1}$ (pH = 2),

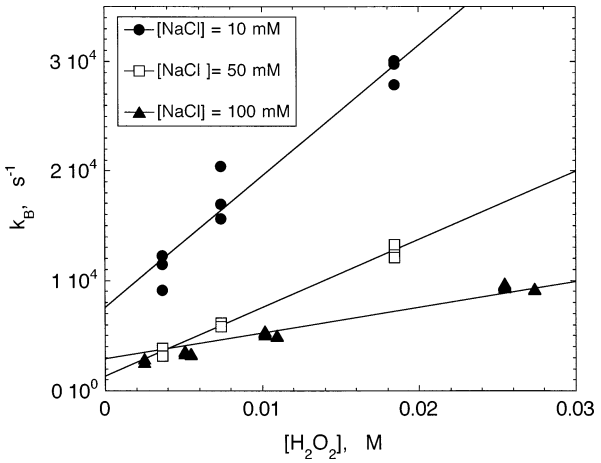

Figure 6. Dependence of k_B on $[H_2O_2]$ for photolysis at 308 nm and for pH = 2. The solid lines are unweighted linear least-squares fits. The $\pm 1\sigma$ statistical errors are about the same size as the data points.

TABLE 3: Some of the Data Used in the Least-Squares Analysis of k_B[a]

		eq 4	
$[Cl^-] \times 10^4$ (M)	runs	intercept $\times 10^{-3}$ (s^{-1})	slope $\times 10^{-7}$ ($M^{-1}\,s^{-1}$)
2.0	16	3.03 ± 0.01	4.32 ± 0.01
4.0	16	1.71 ± 0.01	3.28 ± 0.01
6.0	16	1.40 ± 0.01	2.19 ± 0.01
8.0	16	1.15 ± 0.01	1.92 ± 0.01
10.0	16	1.39 ± 0.01	1.58 ± 0.01

[a] Statistical uncertainties ($\pm 1\sigma$) were obtained from an unweighted least-squares analysis, as described in the text.

corresponding to $k_4K_3 = (1.80 \pm 0.03) \times 10^{10}\ M^{-1}\ s^{-1}$. This result is in good agreement with literature values, despite the fact that different experimental techniques were used.[16,42,55,89] It is also in good agreement with the rate constants deduced from $Cl_2^{\bullet-}$ yields (at higher pH) in our companion study of $HO^\bullet$ quantum yields.[35] All of these studies support the conclusion that $k_{-3} \gg k_4[H^+]$ and, hence, $k_g = K_3k_4[H^+]$.

4.3. Analysis Based on k_B. When equilibrium 5 is maintained at low $[H_2O_2]$, the fitted rate constant k_B is given by eq IV, which has a linear dependence on $[H_2O_2]$. As $[H_2O_2]$ is increased still more, k_B deviates from linearity because reactions 5 and −5 are no longer dominant. To obtain the information on the $Cl_2^{\bullet-}$ decay rate constants, only data in the range of linearity are used to plot k_B vs $[H_2O_2]$ in Figure 6 (only some of the data are shown). The weighted linear least-squares fits of these plots generated sets of intercepts and slopes, some of which are listed in Table 3. For example, in the experiments carried out at 248 nm photolysis, $[H_2O_2]$ ranged from 10^{-4} to 10^{-3} M.

According to eq IV, the intercept and slope of each line in Figure 6 depend on $[Cl^-]$ as follows, as long as $[H_2O_2]$ is not too high:

$$I = \frac{k_8[H_2O]K_5[Cl^-] + k_{-4}[H_2O]}{K_5[Cl^-] + 1} \qquad \text{(Va)}$$

and

$$S = \frac{k_9K_5[Cl^-] + k_{10}}{K_5[Cl^-] + 1} \qquad \text{(Vb)}$$

According to the literature, equilibrium constant K_5 is in the range of $1.4-1.9 \times 10^5\ M^{-1}$.[16,25] Therefore, $K_5[Cl^-]$ is much

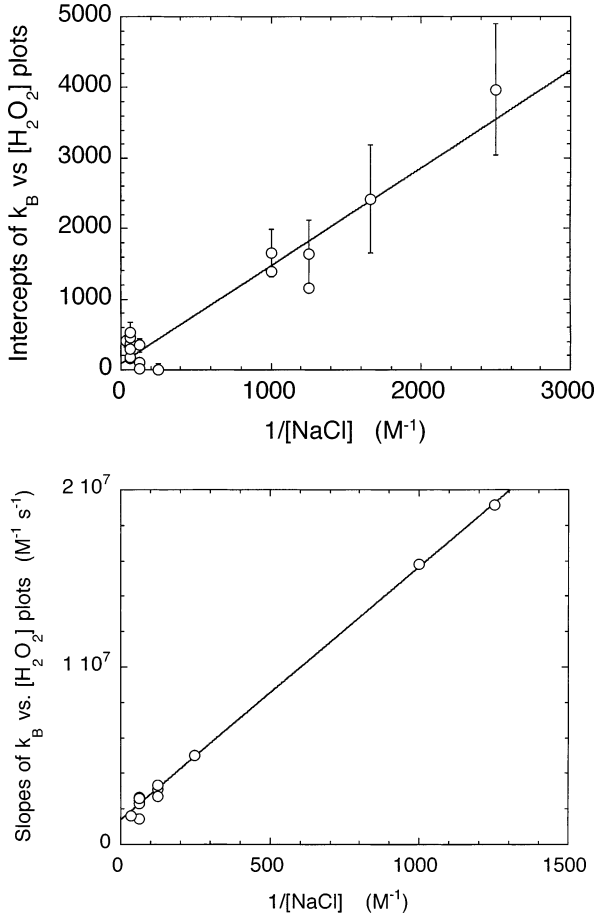

Figure 7. (a) Plot of intercepts (from k_B vs $[H_2O_2]$) vs 1/[NaCl] (see eq Va). The solid line is an unweighted, unconstrained linear least-squares fit. The error bars show $\pm 1\sigma$ statistical errors (note that many data points have uncertainties about the same size as the plotted points or smaller). (b) The plot of S (slopes from k_B vs $[H_2O_2]$) vs 1/[NaCl] (see eq Vb). The open circles are the slopes. The solid line is an unweighted, unconstrained linear least-squares fit. The error bars show $\pm 1\sigma$ statistical errors, although the least-squares fits were performed with equal weighting of data points (note that many data points have uncertainties smaller than the size of the plotted points).

greater than unity when $[Cl^-] > 10^{-4}$ M and eq V simplifies to

$$I = \frac{k_{-4}[H_2O]}{K_5[Cl^-]} + k_8[H_2O] = \frac{S_I}{[Cl^-]} + I_I \qquad \text{(VIa)}$$

and

$$S = \frac{k_{10}}{K_5[Cl^-]} + k_9 = \frac{S_S}{[Cl^-]} + I_S \qquad \text{(VIb)}$$

where $S_I = k_{-4}[H_2O]/K_5$, $I_I = k_8[H_2O]$, $S_S = k_{10}/K_5$, and $I_S = k_9$. Note that the approximations that lead to this expression are less restrictive than those that lead to eq IV: it is only required that $k_5[Cl^-]$ is significantly greater than the other terms in the denominator of eq III and k_{-5} is greater than $k_8[H_2O]$ and $k_9[H_2O_2]$. Thus, eq VI is applicable at higher $[H_2O_2]/[Cl^-]$ ratios than are appropriate for eq IV. The slope (S) and intercept (I) are plotted in Figure 7a,b as functions of $1/[Cl^-]$. The slopes and intercepts of the lines in Figure 7a,b correspond to S_I, S_S and I_I, I_S, respectively. An unweighted linear least-squares analysis gives the results presented in Table 4.

If the mechanism is substantially correct, eq III will be applicable at higher H_2O_2 concentrations, where k_B is no longer

TABLE 4: Results from k_B Analysis at 297 ± 2 K[a]

eq V	eq VI	directly measured results
I	S_I	$k_{-4}[H_2O]/K_5 = (1.4 \pm 0.1)$ M s^{-1}
	I_I	$k_8[H_2O] \leq 100$ M^{-1} s^{-1}
S	S_S	$k_{10}/K_5 = (1.4 \pm 0.2) \times 10^4$ s^{-1}
	I_S	$k_9 = (1.4 \pm 0.2) \times 10^6$ M^{-1} s^{-1}

[a] Statistical uncertainties ($\pm 1\sigma$) were obtained from an unweighted least-squares analysis, as described in the text.

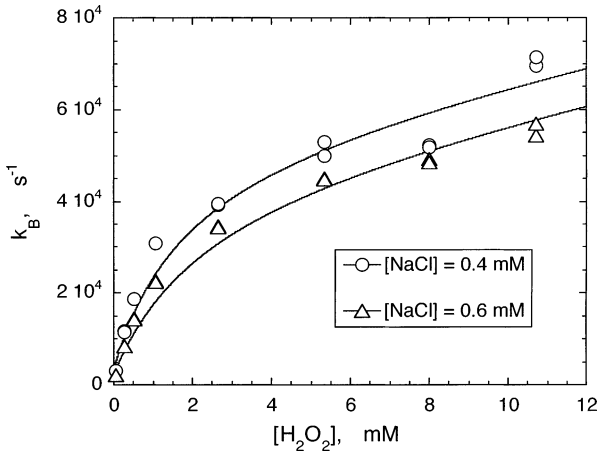

Figure 8. Dependence of k_B on $[H_2O_2]$ at pH = 2. The solid lines are unweighted nonlinear least-squares fits by eq III. The open circles are [NaCl] = 4.0×10^{-4} M, and the open triangles are [NaCl] = 6.0×10^{-4} M. The $\pm 1\sigma$ statistical errors are about the same size as the data points (note that many data points have uncertainties smaller than the size of the plotted points).

a linear function of $[H_2O_2]$. Results for k_B at higher H_2O_2 concentrations are shown in Figure 8. By using the results in Table 4 along with those obtained from the analysis of k_A, all of the rate parameters in eq III are known, except for k_5 and k_{-5}. Rate constant k_5 appears in eq III as a multiplier for $[Cl^-]$. At low $[Cl^-]$, the terms involving k_5 are small relative to the other terms and k_B is relatively insensitive to the specific values chosen for k_5. In contrast, rate constant k_{-5} does not depend on $[Cl^-]$ and k_B remains sensitive to its value. The same general approach was used by Buxton et al.,[25] although the reaction systems are somewhat different.

To assess whether eq III describes the experimental data, we adopted as a trial value for k_5 the recent result $k_5 = (8.5 \pm 0.7) \times 10^9$ M^{-1} s^{-1} reported by Buxton et al.[25] and fitted the data shown for k_B in Figure 8 by a nonlinear least-squares analysis in order to determine k_{-5}. It is apparent in the figure that the experimental results are fitted reasonably well by eq III when $k_{-5} = (5.2 \pm 0.3) \times 10^4$ s^{-1}. We repeated the least-squares analysis using assumed values of k_5 in the range of 1×10^9 to 40×10^9 M^{-1} s^{-1}, which covers a range far wider than the experimental uncertainty in k_5; in no case did the fitted value of k_{-5} vary by more than 5%. The value determined for k_{-5} is affected by much less than 1% by the ~10% experimental uncertainty in k_5. Thus, the fitted value of $k_{-5} = (5.2 \pm 0.3) \times 10^4$ s^{-1} is essentially a direct result of the present experiments.

4.4. Kinetics of $Cl_2^{\bullet-}$ at High $[Cl^-]$. A typical time profile of the formation and decay of $Cl_2^{\bullet-}$ when the chloride concentration is greater than 1×10^{-3} M (at low pH) exhibits a rising portion that is almost instantaneous as compared to the decaying portion. Under these conditions, the conversion of $HO^\bullet$ radical to produce $Cl_2^{\bullet-}$ is almost quantitative and the decay has contributions from both first-order and second-order processes, as described above. As $[Cl^-]$ increases, so does the contribution of second-order processes to the decay of $Cl_2^{\bullet-}$.

At high enough [Cl^-], the second-order decay is dominant, as in previous studies.[48,49]

Although the second-order decay of $Cl_2^{\bullet-}$ is not the focus of the present study, an analysis was carried out using mixed first- and second-order kinetics[48,49] in order to extract values for $2k_6/\epsilon$, where ϵ is the molar extinction coefficient of $Cl_2^{\bullet-}$. At the monitoring wavelength of 364 nm, we found in paper III that $\epsilon(Cl_2^{\bullet-}, 364\ nm) = 7000 \pm 700\ cm\ s^{-1}$ (base 10).[35] In the present work, we analyzed a total of 325 runs using mixed first- and second-order kinetics and obtained $2k_6 = (1.9 \pm 0.2) \times 10^9\ M^{-1}\ s^{-1}$. This result compares well with that found in paper III, where the reaction was investigated more thoroughly and where we obtained $2k_6 = (1.8 \pm 0.1) \times 10^9\ M^{-1}\ s^{-1}$.[31]

Reported values for $2k_6/\epsilon$ fall into the fairly wide range from 0.5×10^5 to $14 \times 10^5\ cm\ s^{-1}$. Some of this variation is due to the use of different monitoring wavelengths, but large systematic errors must also be present. Our result is in good agreement with recent measurements by both laser flash photolysis and pulse radiolysis.[19,47,48,62−65] Although reactions 6 and 7 are included in Table 1, neither is important under most of the conditions used in this study. See paper III for a more detailed discussion.[31]

5. Discussion

5.1. Ionic Strength Effects. Reactions taking place in the aqueous phase are affected by the ionic strength of the medium according to the Debye−Hückel−Bronsted−Davies semiempirical theory[33,90−92]

$$\log_{10}\frac{k_\mu}{k_0} = 2Z_1Z_2A\left\{\frac{\mu^{1/2}}{1+\mu^{1/2}}\right\} - b\mu \qquad \text{(VII)}$$

where k_μ and k_0 are the rate constants at ionic strength μ and 0, respectively, Z_1 and Z_2 are the ionic charges, A is the Debye−Hückel constant ($A = 0.509$ at 298 K), and b is an empirical constant in the range of ∼0.2−0.3 for the few systems that have been studied in sufficient detail.[91,93]

Rate constants are reported in this paper both with and without ionic strength adjustments estimated by using eq VII with $b = 0$. Because almost all of the present experiments were carried out with [NaCl] < 1 mM and pH ≈ 2, the ionic strength of the solutions (∼0.01 M) was not varied significantly. Only two reactions in Table 1 are expected to be affected significantly by ionic strength effects: reactions 4 and 6. None of the other reaction rate constants is affected significantly by the ionic strength, because the corresponding reactants do not include two ions. In experiments reported elsewhere for a wide range of ionic strengths (see paper III for details),[31,34,35] the adjustments to reaction 6, which involve two negative ions, are given by the rate constant ratio $k_6/k_6^0 = 1.3$ at $\mu = 0.01$ M, in good agreement with the value $k_6/k_6^0 = 1.24$ obtained from eq VII with $b = 0$. For reaction 4, which involves oppositely charged ions, eq VII predicts $k_4/k_4^0 = 0.8$. This ionic strength correction also affects equilibrium constant K_4, as noted in Table 1.

5.2. Rate Constants and Equilibrium Constants. The final results obtained from least-squares analysis of the experimental data are summarized in Tables 2 and 4. Several individual rate constants were extracted directly from the data, while other quantities obtained directly are in the form of rate constant ratios. In the first subsection, we will discuss the individual rate constants that were directly extracted; in the subsequent subsections, we employ additional information from the literature in order to extract individual rate constants from the measured rate constant ratios.

5.2.1. Rate Constants Measured Directly. Reaction rate constant k_2 for the reaction of $HO^\bullet$ radicals with H_2O_2 has been measured previously both by direct methods and competition methods. The three previous direct measurements[78−80] range from 1.2×10^7 to $4.5 \times 10^7\ M^{-1}\ s^{-1}$. Competition methods have produced rate constants ranging from 1.7×10^7 to $8.8 \times 10^7\ M^{-1}\ s^{-1}$, as described in paper IV.[32] The present determination of $k_2 = (4.2 \pm 0.2) \times 10^7\ M^{-1}\ s^{-1}$ is consistent with the average of all measurements (including the present work), which is recommended,[32] $k_2 = (3.2 \pm 1.5) \times 10^7\ M^{-1}\ s^{-1}$.

Reactions 8 and 9 describe the attack by $Cl_2^{\bullet-}$ on H_2O and H_2O_2, respectively. Previous measurements[25,47,48] of this rate constant are higher than the recent one by Jacobi et al.[49] and that of the present work. Jacobi et al.[49] compared their result with the earlier works by McElroy[48] and Wagner et al.[47] and provided possible reasons for the discrepancy. Our result is consistent with that of Jacobi et al.[49] Indeed, k_8 is much slower than previously thought. Recently, however, Buxton et al.[25] found a result similar to that of McElroy.[48] The reason for this discrepancy is not known. Despite this disagreement on k_8, it is still clear that the reaction is slow and makes a negligible contribution to the overall decay of $Cl_2^{\bullet-}$.

Three previous measurements of rate constant k_9 have been reported that are scattered over a wide range: 4.1×10^4 to $7.0 \times 10^5\ M^{-1}\ s^{-1}$.[67−69] The result obtained in the present work ($k_9 = (1.4 \pm 0.2) \times 10^6\ M^{-1}\ s^{-1}$) is about a factor of 2 times that of the highest value reported previously, but the uncertainty associated with the present value is relatively small. Considering the wide range of the previously reported results, the present result is certainly reasonable.

5.2.2. k_5, k_{-5}, and K_5 for $Cl^\bullet + Cl^- \leftrightarrow Cl_2^{\bullet-}$. The equilibrium between $Cl^\bullet$, Cl^-, and $Cl_2^{\bullet-}$ is extremely important in governing the overall reactivity of systems that contain solvated Cl atoms and $Cl_2^{\bullet-}$. This is because $Cl^\bullet(aq)$ is a stronger oxidizer and reacts more rapidly than $Cl_2^{\bullet-}$. The equilibrium constant K_5 is necessary for the estimation of the relative concentrations of [$Cl^\bullet$] and [$Cl_2^{\bullet-}$]. Until recently, even the order of magnitude of K_5 was controversial.[16,18,25,27] Jayson et al. were the first to report a value for the equilibrium constant: $K_5 = 1.9 \times 10^5\ M^{-1}$.[16] Although their value has been used widely, a large uncertainty is attached, e.g., 1.4×10^5 to $\sim 2.8 \times 10^5\ M^{-1}$. The extremely low value ($K_5 = 18\ M^{-1}$) reported by Wu et al.[18] was discounted by Wagner et al.,[47] since $Cl_2^{\bullet-}$ would not be detectable at low [Cl^-], contrary to the measurements. The determination by Adams et al.[27] ($K_5 = 4700\ M^{-1}$) was in error, as explained by Buxton et al.,[25] who reported a new measurement: $K_5 = (1.4 \pm 0.1) \times 10^5\ M^{-1}$, where the small uncertainty reflects only the precision of the measurement. To help untangle these disagreements, we can employ directly measured values for rate constants k_5 and k_{-5} to calculate the equilibrium constant: $K_5 = k_5/k_{-5}$. In the following, we summarize the determinations of k_5 and k_{-5}.

5.2.2.1. Forward Rate Constant k_5. The value of k_5 has been determined in several previous studies.[16,25,45,47,53,94] Jayson et al.[16] reported the value of $k_5 = 2.1 \times 10^{10}\ M^{-1}\ s^{-1}$; however, this result was not determined experimentally but was calculated by assuming diffusion control. In fact, they reported a single measured pseudo-first-order rate constant of $4.1 \times 10^6\ s^{-1}$ when the concentrations of hydrogen ions and chloride ions were 1 and 10^{-3} M, respectively.[16] The corresponding value for $k_5 = 4.1 \times 10^9\ M^{-1}\ s^{-1}$ is only ∼20% of the diffusion limit. It is unclear why they preferred the assumed diffusion-controlled rate constant to the experimental value.

TABLE 5: Direct Determinations of k_5 at Room Temperature[a]

k_5 (M^{-1} s^{-1} × 10^{-9})	method[b]	photolysis λ (nm)	probe λ (nm)	pH	year	ref
4.1[c]	PR		340	0	1973	16
21	estimated		340	0	1973	16
6.5 ± 0.9	LFP	308	360	10.0	1985	45
8.0 ± 0.8	LFP	248	340	~3.5	1985	53
8	LFP		340	<5.5	1986	47
19.2	LFP	193	340	NA[d]	1993	94
8.5 ± 0.7	LFP	193	340	NA[d]	1998	25
7.8 ± 0.8	recommended				2001	this work

[a] Rate constants are listed as they appeared in the original papers and have not been extrapolated to zero ionic strength. [b] PR, pulse radiolysis; LFP, laser flash photolysis. [c] See text for explanation. [d] Experimental conditions not available.

Kläning and Wolff[45] measured k_5 directly by generating $Cl_2^{\bullet-}$ by laser flash photolysis of ClO^- and Cl^- under alkaline conditions at 308 nm and monitoring the optical density (OD) of $Cl_2^{\bullet-}$ at 360 nm. Under their conditions, the formation of $Cl_2^{\bullet-}$ is in competition with several other reactions. From a least-squares analysis of their data, they determined that $k_5 = 6.5 \times 10^9$ M^{-1} s^{-1} but did not report the uncertainty.

Nagaranjan and Fessenden[53] generated $Cl_2^{\bullet-}$ by laser flash photolysis of aqueous Cl^- and $S_2O_8^{2-}$ at 248 nm and then used a subsequent photolysis pulse at 355 or 337 nm to photodissociate $Cl_2^{\bullet-}$. The dissociation of the $Cl_2^{\bullet-}$ (monitored at 340 nm) results in a "bleach" and a subsequent exponential recovery back to the original absorption level. The plot of the recovery rate of $Cl_2^{\bullet-}$ vs $[Cl^-]$ was analyzed by least-squares to determine $k_5 = (8.0 \pm 0.8) \times 10^9$ M^{-1} s^{-1}. They reported an estimated 10% error.

Wagner et al.[47] also used a delayed second laser to photolyze $Cl_2^{\bullet-}$ and monitor its relaxation, but they gave no experimental details. Their result ($k_5 = 8.0 \times 10^9$ M^{-1} s^{-1}) agrees exactly with Nagaranjan and Fessenden,[53] but they did not report an associated uncertainty.

Iwata and Yamanaka[94] used laser flash photolysis of Cl^- solution at 193 nm to generate $Cl_2^{\bullet-}$. The absorption signal obtained at 340 nm was the sum of contributions from both $Cl^\bullet$ and $Cl_2^{\bullet-}$. Because the time constant of $Cl^\bullet$ is much faster than the detection limit in their experiments, they assumed that the rate of production of $Cl^\bullet$ was proportional to the time-dependent laser fluence during the laser pulse. With these assumptions, they fitted the experimental data to obtain the quantum yield of $Cl^\bullet$, the formation rate of $Cl_2^{\bullet-}$, and the molar extinction coefficients of $Cl^\bullet$ and $Cl_2^{\bullet-}$. They found that $k_5 = 1.92 \times 10^{10}$ M^{-1} s^{-1} but did not report the uncertainties.[94]

Buxton et al.[25] determined k_5 directly by using laser flash photolysis of Cl^-(aq) at 193 nm and monitoring the growth of $Cl_2^{\bullet-}$ at 340 nm. Because there were no competing reactions, the rate of $Cl_2^{\bullet-}$ growth followed pseudo-first-order kinetics and gave $k_5 = (8.5 \pm 0.7) \times 10^9$ M^{-1} s^{-1}.[25] The uncertainty that they reported is most likely the statistical precision obtained in the least-squares fits. Note that Iwata et al.[94] and Buxton et al.[25] employed virtually identical methods but obtained results that differ by a factor of 2. The measurement of Buxton et al. is in good agreement with the others described above. All of these direct determinations of k_5 are listed in Table 5.

The direct laser flash photolysis of Cl^- is probably the best way to determine k_5. First, the chemical system does not contain species that compete with reaction 5. Second, the pseudo-first-order fit of the observed formation rate constant requires few parameters; therefore, there is less potential correlation among fitted parameters. On the basis of these considerations, we recommend the unweighted average of the direct determinations by Kläning and Wolff,[45] Nagaranjan and Fessenden,[53] Wagner et al.,[47] and Buxton et al.:[25] $k_5 = (7.8 \pm 0.8) \times 10^9$ M^{-1} s^{-1}.

TABLE 6: Determinations of k_{-5} at Room Temperature[a]

k_{-5} (s^{-1})	method[b]	pH	year	ref
$(1.1 \pm 0.4) \times 10^5$	indirect	0	1973	16
7.6×10^5	computer simulation	7	1977	58
$(6.0 \pm 0.5) \times 10^4$	PR	5−6	1998	25
$(5.2 \pm 0.3) \times 10^4$	LFP	2	2001	this work
$(5.7 \pm 0.4) \times 10^4$	recommended		2001	this work

[a] Rate constants are listed as they appeared in the original papers and have not been extrapolated to zero ionic strength. [b] PR, pulse radiolysis; LFP, laser flash photolysis.

5.2.2.2. Reverse Rate Constant k_{-5}. The few results available for reaction −5 are summarized in Table 6. The earliest value reported for k_{-5} was by Jayson et al.,[16] who obtained $k_{-5} = (1.1 \pm 0.4) \times 10^5$ s^{-1} indirectly from their assumed diffusion-controlled value for k_5 and their measured value of equilibrium constant $K_5 = 1.9 \times 10^5$ M^{-1}. Their method for determining K_5 is described below. The actual experimental uncertainty in their value for K_5 ranges from 1.4×10^5 to 2.8×10^5 M^{-1}, which seriously affects the potential accuracy of k_{-5}.

In a pulse radiolysis experiment, Zansokhova et al.[58] reported $k_{-5} = 7.6 \times 10^5$ M^{-1} and $2k_6 = 1.7 \times 10^{10}$ M^{-1} s^{-1} as the best combination of the modeled and experimental relationship between $[Cl_2^{\bullet-}]_{max}$ and dose per pulse. The accuracy of k_{-5} is correlated with that of $2k_6$, and Zansokhova et al. obtained a value for $2k_6$ that is substantially larger than found in recent measurements.[31,48,64,65] It is possible that the high result is due to correlations in the numerical analysis of their data. Therefore, it is likely that the accuracy of k_{-5} is affected by the high value for $2k_6$.

Recently, Buxton et al.[25] determined k_{-5} by examining the decay of $Cl_2^{\bullet-}$ by pulse radiolysis of an aqueous solution containing 1×10^{-3} M $Na_2S_2O_8$, chloride ions ($[Cl^-] \geq 1 \times 10^{-3}$ M) and 2-methyl-propan-2-ol (*t*-BuOH). Chlorine atom and dichloride radical anion readily react with the hydroxyl group of *t*-BuOH. These reactions compete with the reactions of $Cl^\bullet$ and $Cl_2^{\bullet-}$ with H_2O. Buxton et al. found that the observed pseudo-first-order decay rate constant of $Cl_2^{\bullet-}$ departed from linearity as the concentration of *t*-BuOH was increased, due to the finite rate of reaction 5 in competition with the reactions with *t*-BuOH.[25] By using their measured value of k_5 in a least-squares procedure, they determined that $k_{-5} = (6.0 \pm 0.5) \times 10^4$ s^{-1}. (We used the same procedure for fitting k_B at higher $[H_2O_2]$, as described above.)

The result obtained in the present work ($k_{-5} = (5.2 \pm 0.3) \times 10^4$ s^{-1}) is not sensitive to the value of k_5, as discussed above. The technique used here is virtually the same as that used by Buxton et al., although the reference reactions were different. Because the likely errors are of the same magnitude, we conclude that the best unbiased estimate for k_{-5} is the unweighted average of the present measurement and that of Buxton et al.:[25] $k_{-5} = (5.7 \pm 0.4) \times 10^4$ s^{-1}.

5.2.2.3. Equilibrium Constant K_5. Jayson et al.[16] assumed that the optical absorption due to $Cl_2^{\bullet-}$ had reached its maximum possible value when [NaCl] = 0.01 M and $[HClO_4]$ = 0.01 M. They then measured the absorption due to $Cl_2^{\bullet-}$ under various other conditions of [NaCl] and $[HClO_4]$ and expressed the results as functions of equilibrium constants, i.e., K_3, K_4, and K_5. From among a range of algebraic solutions that described their data, they reported $K_3K_4 = 1.1 \times 10^7$ M^{-1} and $K_5 = 1.9 \times 10^5$ M^{-1}.[16] When all of the algebraic solutions are considered, the possible

TABLE 7: Summary of Results (This Paper) and Recommendations for Rate Constants[a]

reaction	results (this paper)	recommendations	recommendation ref
1		$\phi_{OH} = 1.0$, independent of λ	35
2	$k_2 = (4.2 \pm 0.2) \times 10^7\ M^{-1}\ s^{-1}$	$k_2 = (3.2 \pm 1.5) \times 10^7\ M^{-1}\ s^{-1}$	this work and 32
3		$k_3 = (4.3 \pm 0.4) \times 10^9\ M^{-1}\ s^{-1}$	16
−3		$k_{-3} = (6.1 \pm 0.8) \times 10^9\ M^{-1}\ s^{-1}$	16
		$K_3 = 0.70 \pm 0.13\ M^{-1}$	16
4	$k_4 = (2.6 \pm 0.6) \times 10^{10}\ M^{-1}\ s^{-1}$	$k_4 = (2.6 \pm 0.6) \times 10^{10}\ M^{-1}\ s^{-1}$	this work
	$k_4^0 = (3.2 \pm 0.7) \times 10^{10}\ M^{-1}\ s^{-1}$	$k_4^0 = (3.3 \pm 0.9) \times 10^{10}\ M^{-1}\ s^{-1}$	
−4	$k_{-4}[H_2O] = (2.0 \pm 0.2) \times 10^5\ s^{-1}$[a]	$k_{-4}[H_2O] = (1.8 \pm 0.5) \times 10^5\ s^{-1}$	this work and 31
	$K_4 = (7.2 \pm 1.6) \times 10^6$	$K_4 = (7.2 \pm 1.6) \times 10^6$	this work
	$K_4^0 = (8.8 \pm 2.2) \times 10^6$	$K_4^0 = (8.8 \pm 2.2) \times 10^7$	this work
5		$k_5 = (7.8 \pm 0.8) \times 10^9\ M^{-1}\ s^{-1}$	this work
−5	$k_{-5} = (5.2 \pm 0.3) \times 10^4\ s^{-1}$	$k_{-5} = (5.7 \pm 0.4) \times 10^4\ s^{-1}$	this work and 32
		$K_5 = (1.4 \pm 0.2) \times 10^5\ M^{-1}$	this work
6	$k_6 = (9 \pm 1) \times 10^8\ M^{-1}\ s^{-1}$	$k_6 = (9 \pm 1) \times 10^8\ M^{-1}\ s^{-1}$	this work and 31
	$k_6^0 = (7.2 \pm 0.8) \times 10^8\ M^{-1}\ s^{-1}$	$k_6^0 = (7.2 \pm 0.8) \times 10^8\ M^{-1}\ s^{-1}$	
7		$2\,k_7 = (4.2 \pm 0.1) \times 10^9\ M^{-1}\ s^{-1}$	31
8	$k_8[H_2O] < 100\ s^{-1}$	$k_8[H_2O] < 100\ s^{-1}$	this work and 31
9	$k_9 = (1.4 \pm 0.2) \times 10^6\ M^{-1}\ s^{-1}$	$k_9 = (1.4 \pm 0.2) \times 10^6\ M^{-1}\ s^{-1}$	This work
10	$k_{10} = (2.0 \pm 0.3) \times 10^9\ M^{-1}\ s^{-1}$	$k_{10} = (2.0 \pm 0.3) \times 10^9\ M^{-1}\ s^{-1}$	this work
11		$k_{11} = (3.1 \pm 1.5) \times 10^9\ M^{-1}\ s^{-1}$	32
12		$k_{12} = 0.5\ M^{-1}\ s^{-1}$	76
13		$k_{13} = 6.0 \times 10^9\ M^{-1}\ s^{-1}$	106
15		$k_{15} = 9.8 \times 10^5\ M^{-1}\ s^{-1}$	107
16		$k_{16} = 1.0 \times 10^{10}\ M^{-1}\ s^{-1}$	108

[a] In this paper, uncertainties ($\pm 1\sigma$) were obtained from error propagation; ionic strength (μ) $\approx$ 0.01 M unless otherwise noted by a superscript "0" on rate constants that have been adjusted to $\mu = 0$.

range of K_5 is large (i.e., 1.4×10^5 to $2.8 \times 10^5\ M^{-1}$) but Jayson et al. did not explain how they arrived at their preferred value.

The equilibrium constant can also be obtained from the ratio of forward and reverse rate constants. The values recommended here for k_5 and k_{-5}, respectively, are $(7.8 \pm 0.8) \times 10^9\ M^{-1}\ s^{-1}$ and $(5.7 \pm 0.4) \times 10^4\ s^{-1}$. The ratio of these values gives $K_5 = (1.4 \pm 0.2) \times 10^5\ M^{-1}$, where the uncertainty was obtained by propagation of errors. This value is in good agreement with that reported recently by Buxton et al.,[25] as well as that of Jayson et al.,[16] and we recommend it as the best unbiased estimate of the equilibrium constant. With this recommended value for K_5 and the standard reduction potential $E(Cl^{\bullet}/Cl^-) = 2.41$ V,[95] we obtain the standard reduction potential $E(Cl_2^{\bullet -}/2Cl^-) = 2.11$ V, which differs only slightly from the value obtained using the equilibrium constant from Jayson et al. ($E(Cl_2^{\bullet -}/2Cl^-) = 2.09$ V).

5.2.3. k_4, k_{-4}, and K_4 for $ClOH^{\bullet -} + H^+ \rightarrow Cl^{\bullet} + H_2O$. Under the conditions of the present work, "global" rate constant k_g is given to a very good approximation by $k_g = K_3 k_4 [H^+]$, as discussed above. The value obtained in the present work for k_g is consistent with results reported by Jayson et al.[16] and Anbar et al.[42] From the present experimental results at pH = 2 and the equilibrium constant $K_3 = 0.70$ mpm$\pm$ 0.13 M^{-1} reported by Jayson et al.,[16] we obtain $k_4 = (2.6 \pm 0.6) \times 10^{10}\ M^{-1}\ s^{-1}$. Note that the only measurement of K_3 is that of Jayson et al.[16] Also note that the rate constant k_4 is subject to ionic strength effects. As discussed above in section 5.1, the Debye−Hückel theory predicts that at infinite dilution, rate constant k_4 would be about 20% higher than the value obtained in our experiments, where the ionic strength is ~0.01 M.

The value of k_{-4} is often expressed as a pseudo-first-order rate constant: $k_{-4}^I = k_{-4}[H_2O]$. It is reasonable to compare the ratio of k_{-4}^I/K_5 obtained in various investigations instead of k_{-4}^I reported from various investigations, because the latter is affected by the different values of K_5 adopted by different researchers. The present result of $k_{-4}^I/K_5 = 1.4 \pm 0.1$ M s^{-1}, is in good agreement with previous measurements.[25,45,48,49] On the basis of our recommended value $K_5 = (1.4 \pm 0.2) \times 10^5\ M^{-1}$, we obtain $k_{-4}^I = (2.0 \pm 0.2) \times 10^5\ s^{-1}$.

With the knowledge of k_{-4} and k_4, we can calculate $K_4 = k_4/k_{-4}$. From the values obtained above for the two rate constants, we obtain $K_4 = (7.2 \pm 1.6) \times 10^6$. Using $k_{-4} = (3.6 \pm 0.4) \times 10^3\ M^{-1}\ s^{-1}$ obtained in this work and the Debye−Hückel theory (eq VII) to estimate k_4^0 at zero ionic strength, we obtain $k_4^0 = (3.2 \pm 0.7) \times 10^{10}\ M^{-1}\ s^{-1}$ and $K_4^0 = (8.8 \pm 2.2) \times 10^6$. Both values are slightly lower than the value reported by Jayson et al.,[16] which corresponds to an ionic strength of unity.

5.2.4. k_{10} for the Reaction $Cl^{\bullet} + H_2O_2 \rightarrow H^+ + Cl^- + HO_2^{\bullet}$. The chemistry of the chlorine atom in aqueous solution is analogous to that of the hydroxyl radical, which is a pseudo-halogen (isoelectronic with fluorine atom). Both $HO^{\bullet}$ and $Cl^{\bullet}$ are efficient hydrogen atom abstractors.[14] Although the reaction of $Cl^{\bullet}$ with H_2O_2 has a relatively large rate constant in the gas phase, the aqueous phase rate constant has not been reported previously. The ratio k_{10}/K_5 obtained from the data in Figure 7b is reported in Table 4. By taking the recommended value $K_5 = (1.4 \pm 0.2) \times 10^5\ M^{-1}$, we obtain $k_{10} = (2.0 \pm 0.3) \times 10^9\ M^{-1}\ s^{-1}$. This result for the reaction in the aqueous phase is about 10 times faster than in the gas phase, where $k_{10}(g) = (2.47 \pm 0.12) \times 10^8\ M^{-1}\ s^{-1}$.[29] It is about 2 orders of magnitude faster than the estimate by Graedel and Goldberg for the aqueous phase.[96] It is not unusual that k_{10} is faster in the aqueous phase than in the gas phase, since solvent plays an important role in modifying the interaction between reacting species.[97,98] In particular, it seems likely that solvation has lowered the activation barrier. This result is yet another illustration that gas phase rate constants do not necessarily provide good quantitative estimates for the solution phase.

6. Conclusions

In the preceding sections, we have described rate and equilibrium constants that were measured directly in the experiments or extracted (with the aid of additional literature data) from measured ratios. We have also evaluated relevant data from our own and from other's experiments. All of the new results are consistent with the chemical mechanism described by Jayson et al.[16] and are gathered together in Tables

1 and 7. In many cases, there is good consistency among measurements from different laboratories, showing that the chemical mechanism is generally well-understood. A few reactions require more study. For example, the equilibrium constant for reaction 3 has only been determined once since the report by Jayson et al.,[16] although the $ClOH^{\bullet-}$ radical is an important intermediate in the reaction involving $HO^{\bullet}$ radicals.

In the present work, reaction 9 was found to be much slower than reaction 10. Both reactions were measured simultaneously for the first time in this work. Both reactions may be important in free radical systems in which hydrogen peroxide plays a role.

Currently, there is intense interest in halogen activation as an explanation for the dramatic depletions of ozone observed in polar regions near the coastline.[1,2,5−7,9,11,12,99−104] It is possible that halogen activation takes place in the marine boundary layer over much of the globe and that the special conditions found in the polar springtime are particularly favorable for observations of the effect. Halogen activation may also take place in the interior of the snowpack.[103] The aqueous free radical reaction mechanism in Table 1 shows that halogen activation can occur as a result of free radical reactions involving chlorine-containing species. Similar reaction mechanisms are found for the other halogens, including bromine, which has been directly implicated in the ozone depletion events mentioned above. Quantitative modeling calculations will be needed to assess the quantitative importance of aqueous free radical reactions in this regard, but it seems likely that they at least will contribute to initiation of halogen activation cycles. In addition, if the principal aqueous free radical chain carriers consist of $Cl_2^{\bullet-}$, $Br_2^{\bullet-}$, and $BrCl^{\bullet-}$, which react to eventually produce gas phase halogens, then the aqueous free radical chain mechanism may contribute significantly to halogen activation during daylight hours (when free radicals are produced by photolysis). A modeling study is needed in order to assess these possibilities.

Acknowledgment. We thank NASA (Upper Atmospheric Research Program) and NSF (Atmospheric Chemistry Division) for financial support of this work. We also thank Robert Huie, Paul Wine, and Anthony Hynes for helpful discussions.

Appendix: $Cl_2^{\bullet-}$ Kinetics

The rise and decay of $[Cl_2^{\bullet-}]$ is described by the mechanism shown in Table 1. For convenience, we will assume quasi-steady state for $[ClOH^{\bullet-}]$, allowing us to combine reactions 3 and 4 to produce global reaction g:

$$HO^{\bullet} + Cl^{-} (+ H^{+}) \rightarrow Cl^{\bullet} + H_2O \qquad \text{(g)}$$

The global forward and reverse rate constants for reaction g are found by a quasi-steady state analysis for $[ClOH^{\bullet-}]$:

$$k_g = \frac{k_3 k_4 [H^+]}{k_{-3} + k_4 [H^+]} \qquad \text{(A.1)}$$

and

$$k_{-g} = \frac{k_{-3} k_{-4}}{k_{-3} + k_4 [H^+]} \qquad \text{(A.2)}$$

Using this global reaction, we can write down the differential equations for $[HO^{\bullet}]$, $[Cl^{\bullet}]$, and $[Cl_2^{\bullet-}]$:

$$\frac{d[Cl^{\bullet}]}{dt} = k_g [^{\bullet}OH][Cl^-] + a[Cl_2^{\bullet-}] - b[Cl^{\bullet}] \qquad \text{(A.3)}$$

$$\frac{d[Cl_2^{\bullet-}]}{dt} = c[Cl^{\bullet}] - f[Cl_2^{\bullet-}] \qquad \text{(A.4)}$$

$$\frac{d[^{\bullet}OH]}{dt} = -k_A [^{\bullet}OH] \qquad \text{(A.5)}$$

where $a = k_{-5}$, $b = k_5[Cl^-] + k_{10}[H_2O_2] + k_{-g}[H_2O]$, $c = k_5[Cl^-]$, $f = k_{-5} + k_8[H_2O] + k_9[H_2O_2]$, and $k_A = k_2[H_2O_2] + k_g[Cl^-]$.

Equation A.6 is obtained by rearrangement of eq A.4

$$[Cl^{\bullet}] = \frac{1}{c}\left(\frac{d[Cl_2^{\bullet-}]}{dt} + f[Cl_2^{\bullet-}]\right) \qquad \text{(A.6)}$$

The derivative of $[Cl^{\bullet}]$ with respect to time is

$$\frac{d[Cl^{\bullet}]}{dt} = \frac{1}{c}\left(\frac{d^2[Cl_2^{\bullet-}]}{dt^2} + f\frac{d[Cl_2^{\bullet-}]}{dt}\right) \qquad \text{(A.7)}$$

By substituting eq A.7 into eq A.3, we obtain

$$\frac{d^2[Cl_2^{\bullet-}]}{dt^2} + \alpha\frac{d[Cl_2^{\bullet-}]}{dt} + \beta[Cl_2^{\bullet-}] = \gamma \cdot e^{-k_A t} \qquad \text{(A.8)}$$

where $\alpha = f + b$, $\beta = bf - ac$, and $\gamma = ck_g[OH]_o[Cl^-]$.

The general solution of the nonhomogeneous differential eq A.8 is[25,105]

$$[Cl_2^{\bullet-}] = C_1 \cdot e^{\lambda_1 t} + C_2 \cdot e^{\lambda_2 t} + \frac{\gamma}{k_A{}^2 - \alpha k_A + \beta} e^{-k_A t} \qquad \text{(A.9)}$$

where C_1 and C_2 are coefficients to be determined from the initial conditions and

$$\lambda_1 = -\frac{1}{2}\{\alpha - \sqrt{\alpha^2 - 4\beta}\},\ \lambda_2 = -\frac{1}{2}\{\alpha + \sqrt{\alpha^2 - 4\beta}\} \qquad \text{(A.10)}$$

From the definitions of α and β, it is possible to show that $\alpha^2 - 4\beta \gg 0$ and therefore, λ_2 is more negative than λ_1. Hence, $\exp(\lambda_2 t)$ becomes negligible rapidly and may be ignored when sufficiently small. This approximation is consistent with the experiments, which show no signs of a third time constant. It is also consistent with the magnitudes calculated from the measured rate constants. In all of the subsequent analyses, we assume that the term containing $\exp(\lambda_2 t)$ can be neglected.

Coefficient C_1 in eq A.9 can be found from the condition that $[Cl_2^{\bullet-}]_0 = 0$ at $t = 0$, and the resulting expression is

$$[Cl_2^{\bullet-}] = \frac{\gamma}{k_A{}^2 - \alpha k_A + \beta}(e^{-k_A t} - e^{\lambda_1 t}) \qquad \text{(A.11)}$$

If we take the definitions for α, β, and γ given above, identify $-\lambda_1$ with rate constant k_B, and write $C = k_5 k_g [Cl^-]^2/(k_A{}^2 - \alpha k_A + \beta)$, eq A.12 can be written

$$[Cl_2^{\bullet-}] = C[^{\bullet}OH]_o\{e^{-k_A t} - e^{-k_B t}\} \qquad \text{(A.12)}$$

where

$$k_A = k_2[H_2O_2] + k_g[Cl^-] \quad \text{(A.13)}$$

and

$$k_B = \{(k_8[H_2O] + k_9[H_2O_2])k_5[Cl^-] + (k_{-g}[H_2O] + k_{10}[H_2O_2])(k_{-5} + k_8[H_2O] + k_9[H_2O_2])\}\Big/\{k_5[Cl^-] + k_{-5} + k_{-g}[H_2O] + k_{10}[H_2O_2] + k_8[H_2O] + k_9[H_2O_2]\} \quad \text{(A.14)}$$

When experimental conditions are controlled so that the rates of reaction 5 and reaction −5 dominate the formation and the loss, respectively, of $Cl_2^{\bullet-}$, then eq A.14 simplifies to the following expression:

$$k_B' = \left\{\frac{k_8K_5[Cl^-] + k_{-g}}{K_5[Cl^-] + 1}\right\}[H_2O] + \left\{\frac{k_9K_5[Cl^-] + k_{10}}{K_5[Cl^-] + 1}\right\}[H_2O_2] \quad \text{(A.15)}$$

References and Notes

(1) Barrie, L. A.; Bottenheim, J. W.; Schnell, R. C.; Crutzen, P. J.; Rasmussen, R. A. *Nature* **1988**, *334*, 138.
(2) Fan, S.-M.; Jacob, D. J. *Nature* **1992**, *359*, 522.
(3) Mozurkewich, M. *JGR* **1995**, *100*, 14199.
(4) Singh, H. B.; Gregory, G. L.; Anderson, B.; Browell, E.; Sachse, G. W.; Davis, D. D.; Crawford, J.; Bradshaw, J. D.; Talbot, R.; Blake, D. R.; Thornton, D.; Newll, R.; Merrill, J. *JGR* **1996**, *101*, 1907.
(5) Vogt, R.; Crutzen, P. J.; Sander, R. *Nature* **1996**, *383*, 327.
(6) Oum, K. W.; Lakin, M. J.; DeHaan, D. O.; Brauers, T.; Finlayson-Pitts, B. J. *Science* **1998**, *279*, 74.
(7) Oum, K. W.; Lakin, M. J.; Finlayson-Pitts, B. J. *Geophys. Res. Lett.* **1998**, *25*, 3923.
(8) Dickerson, R. R.; Rhoads, K. P.; Carsey, T. P.; Oltmans, S. J.; Burrows, J. P.; Crutzen, P. J. *J. Geophys. Res.* **1999**, *104*, 21385.
(9) Platt, U.; Moortgat, G. K. *J. Atmos. Chem.* **1999**, *34*, 1.
(10) Behnke, W.; Elend, M.; Krüger, U.; Zetzsch, C. *J. Atmos. Chem.* **1999**, *34*, 87.
(11) Jacob, D. J. *Atmos. Environ.* **2000**, *34*, 2131.
(12) Seinfeld, J. H. *Science* **2000**, *288*, 285.
(13) Knipping, E. M.; Lakin, M. J.; Foster, K. L.; Jungwirth, P.; Tobias, D. J.; Gerber, R. B.; Dabdub, D.; Finlayson-Pitts, B. J. *Science* **2000**, *288*, 301.
(14) Graedel, T. E.; Weschler, C. J. *Rev. Geophys. Space Phys.* **1981**, *19*, 505.
(15) Kraljić, I. *Int. J. Radiat. Phys. Chem.* **1970**, *59*, 59.
(16) Jayson, G. G.; Parsons, B. J.; Swallow, A. J. *J. Chem. Soc., Faraday Trans. 1* **1973**, *69*, 1597.
(17) Kim, K.-J.; Hamill, W. H. *J. Phys. Chem.* **1976**, *80*, 2325.
(18) Wu, D.; Wong, D.; Bartolo, B. D. *J. Photochem.* **1980**, *14*, 303.
(19) Slama-Schwok, A.; Rabani, J. *J. Phys. Chem.* **1986**, *90*, 1176.
(20) Gilbert, B. C.; Stell, J. K.; Peet, W. J.; Radford, K. J. *J. Chem. Soc., Faraday Trans. 1* **1988**, *84*, 3319.
(21) Wine, P. H.; Tang, Y.; Thorn, T. P.; Wells, J. R. *J. Geophys. Res.* **1989**, *94*, 1085.
(22) Huie, R. E.; Clifton, C. L.; Kafafi, S. A. *J. Phys. Chem.* **1991**, *95*, 9336.
(23) Henbest, K.; Douglas, P.; Garley, M. S.; Mills, A. *J. Photochem. Photobiol. A: Chem.* **1994**, *80*, 299.
(24) Herrmann, H.; Jacobi, H.-W.; Reese, A.; Zellner, R. Laboratory studies of small radicals and radical anions of interest for tropospheric aqueous phase chemistry: The reactivity of SO_4^-; *EUROTRAC Symposium '96*, 1996.
(25) Buxton, G. V.; Bydder, M.; Salmon, G. A. *J. Chem. Soc., Faraday Trans. 1* **1998**, *94*, 653.
(26) Buxton, G. V.; Bydder, M.; Salmon, G. A. *Phys. Chem. Chem. Phys.* **1999**, *1*, 269.
(27) Adams, D. J.; Barlow, S.; Buxton, G. V.; Malone, T. N.; Salmon, G. A. *J. Chem. Soc., Faraday Trans. 1* **1995**, *91*, 3303.
(28) Liu, Y.; Pimentel, A. S.; Antoku, Y.; Giles, B. J.; Barker, J. R. *J. Phys. Chem. A* **2002**, *106*, 11075.
(29) Atkinson, R.; Baulch, D. L.; Cox, R. A.; Hampson, R. F. J.; Kerr, J. A.; Rossi, M. J.; Troe, J. *J. Phys. Chem. Ref. Data* **2000**, *29*, 167.
(30) Yu, X.-Y.; Barker, J. R. *J. Phys. Chem. A* **2003**, *107*, 1325.
(31) Yu, X.-Y.; Bao, Z.-C.; Barker, J. R. *J. Phys. Chem. A* **2003**, manuscript in preparation.
(32) Yu, X.-Y.; Barker, J. R. **2003**, manuscript in preparation.
(33) Bao, Z.-C.; Barker, J. R. *J. Phys. Chem.* **1996**, *100*, 9780.
(34) Bao, Z.-C. Temperature and ionic strength dependence of some sulfate [SO_4(aq)] and dichloride [Cl_2(aq)] radical reactions. Ph.D., University of Michigan, 1997.
(35) Yu, X.-Y. Kinetics of Free Radical Reactions Generated by Laser Flash Photolysis of OH + Cl^- and SO_4^- + Cl^- in the Aqueous Phase—Chemical Mechanism, Kinetics Data and Their Implications. Ph.D. (Chemistry), The University of Michigan, 2001.
(36) Buxton, G. V.; McGowan, S.; Salmon, G. A.; Williams, J. E.; Wood, N. D. *Atmos. Environ.* **1996**, *30*, 2483.
(37) de Violet, P. F. *Rev. Chem. Intermed.* **1981**, *4*, 121.
(38) White, J. U. *J. Opt. Soc. Am.* **1942**, *32*, 285.
(39) Synergy. *KaleidaGraph*, 3.51 ed.; Synergy Software: 2001.
(40) Press, W. H.; Teukolsky, S. A.; Vetterling, W. T.; Flannery, B. P. *Numerical Recipes in FORTRAN. The Art of Scientific Computing*, 2nd ed.; Cambridge University Press: Cambridge, 1992.
(41) Boltz, D. F.; Howell, J. A. *Colorimetric Determination of Nonmetals*, 1st ed.; New York Interscience: New York, 1958.
(42) Anbar, M.; Thomas, J. K. *J. Phys. Chem.* **1964**, *68*, 3829.
(43) Sweet, J. P.; Thomas, J. K. *J. Phys. Chem.* **1964**, *68*, 1363.
(44) Zhestkova, T. P.; Pikaev, A. K. *Bull. Akad. Nauk SSSR, Div. Chem. Sci.* **1974**, *23*, 877.
(45) Kläning, U. K.; Wolff, T. *Ber. Bunsen-Ges. Phys. Chem.* **1985**, *89*, 243.
(46) Navaratnam, S.; Parsons, B. J.; Swallow, A. J. *Radiat. Phys. Chem.* **1980**, *15*, 159.
(47) Wagner, I.; Karthäuser, J.; Strehlow, H. *Ber. Bunsen-Ges. Phys. Chem.* **1986**, *90*, 861.
(48) McElroy, W. J. *J. Phys. Chem.* **1990**, *94*, 2435.
(49) Jacobi, H.-W.; Herrmann, H.; Zellner, R. *Ber. Bunsen-Ges. Phys. Chem.* **1997**, *101*, 1909.
(50) Buxton, G. V.; Bydder, M.; Salmon, G. A.; Williams, J. E. *Phys. Chem. Chem. Phys.* **2000**, *2*, 237.
(51) Allen, A. O. *Radiat. Res.* **1964**, Suppl. 4, 54.
(52) Thomas, J. K. *J. Phys. Chem.* **1963**, *67*, 2593.
(53) Nagarajan, V.; Fessenden, R. W. *J. Phys. Chem.* **1985**, *89*, 2330.
(54) Langmuir, M. E.; Hayon, E. *J. Phys. Chem.* **1967**, *71*, 3808.
(55) Ward, J. F.; Kuo, I. Steady state and pulse radiolysis of aqueous chloride solutions of nucleic acid components; Presented at the International Conference sponsored by Argonne National Laboratory, Argonne, IL, 1968.
(56) Patterson, L. K.; Bansal, K. M.; Bogan, G.; Infanta, G. A.; Fendler, E. J.; Fendler, J. H. *J. Am. Chem. Soc.* **1972**, *94*, 9028.
(57) Thornton, A. T.; Laurence, G. S. *J. Chem. Soc. Dalton* **1973**, *8*, 804.
(58) Zansokhova, A. A.; Kabakchi, S. A.; Pikaev, A. K. *High Energy Chem.* **1977**, *11*, 50.
(59) Woods, R. J.; Lesigne, B.; Giles, L.; Ferradini, C.; Pucheault, J. *J. Phys. Chem.* **1975**, *79*, 2700.
(60) Broszkiewicz, R. K. *Bull. Akad. Pol. Sci. Ser. Sci. Chim.* **1976**, *XXIV*, 123.
(61) Gogolev, A. Y.; Makarov, I. E.; Pikaev, A. K. *High Energy Chem.* **1984**, *18*, 390.
(62) Lierse, C.; Sullivan, J. C.; Schmidt, K. H. *Inorg. Chem.* **1987**, *26*, 1408.
(63) Hynes, A. J.; Wine, P. H. *J. Chem. Phys.* **1988**, *89*, 3565.
(64) Huie, R. E.; Clifton, C. L. *J. Phys. Chem.* **1990**, *94*, 8561.
(65) Jacobi, H.-W.; Wicktor, F.; Herrmann, H.; Zellner, R. *Int. J. Chem. Kinet.* **1999**, *31*, 169.
(66) Gilbert, C. W.; Ingalls, R. B.; Swallow, A. J. *Radiat. Phys. Chem.* **1977**, *10*, 221.
(67) Elliot, A. J. *Radiat. Phys. Chem.* **1989**, *34*, 753.
(68) Hasegawa, K.; Neta, P. *J. Phys. Chem.* **1978**, *82*, 854.
(69) Jacobi, H.-W.; Herrmann, H.; Zellner, R. Kinetic investigation of the Cl_2^- radical in the aqueous phase. In *Homogeneous and Heterogeneous Chemical Processes in the Troposphere*; Mirabel, P., Ed.; European Commission: Luxembourg, 1996; p 172.
(70) Haber, F.; Weiss, J. *Proc. R. Soc. London A* **1934**, *147*, 332.
(71) Buxton, G. V. *Trans. Faraday Soc.* **1969**, *65*, 2150.
(72) Sehested, K.; Holcman, J.; Bjergbakke, E.; Hart, E. J. *J. Phys. Chem.* **1982**, *86*, 2066.
(73) Koppenol, W. H.; Butler, J.; van Leeuwen, J. W. *Photochem. Photobiol.* **1978**, *28*, 655.
(74) Melhuish, W. H.; Sutton, H. C. *J. Chem. Soc. Chem. Commun.* **1978**, 970.
(75) Ferradini, C.; Foos, J.; Houee, C.; Pucheault, J. *Photochem. Photobiol.* **1978**, *28*, 697.
(76) Weinstein, J.; Bielski, B. H. J. *J. Am. Chem. Soc.* **1979**, *101*, 58.
(77) Currie, D. J.; Dainton, F. S. *Trans. Faraday Soc.* **1965**, *61*, 1156.

(78) Christensen, H.; Sehested, K.; Corfitzen, H. *J. Phys. Chem.* **1982**, *86*, 1588.
(79) Schwarz, H. A. *J. Phys. Chem.* **1962**, *66*, 255.
(80) Fricke, H.; Thomas, J. K. *Radiat. Res. Suppl.* **1964**, *4*, 35.
(81) Ferradini, C.; Koulkès-Pujo, A. M. *J. Chim. Phys.* **1963**, *60*, 1310.
(82) Thomas, J. K. *Trans. Faraday Soc.* **1965**, *61*, 702.
(83) Greenstock, C. L.; Wiebe, R. H. Kinetic studies of peroxides and peroxy radicals, and their reactions with biological molecules. In *Oxygen and Oxy-radicals in Chemistry and Biology*; Rodgers, M. A. J., Powers, E. L., Eds.; Academic Press Inc.: New York, 1980; p 119.
(84) Baxendale, J. H.; Khan, A. A. *Int. J. Radiat. Phys. Chem.* **1969**, *1*, 11.
(85) Kachanova, Z. P.; Kozlov, Y. N. *Russ. J. Phys. Chem.* **1973**, *47*, 1190.
(86) Hatada, M.; Kraljic, I.; Samahy, A. E.; Trumbore, C. N. *J. Phys. Chem.* **1974**, *78*, 888.
(87) Merényi, G.; Lind, J. S. *J. Am. Chem. Soc.* **1980**, *102*, 5830.
(88) Armstrong, W. A. *Can. J. Chem.* **1969**, *47*, 3737.
(89) Ward, J. F.; Myers, L. S., Jr. *Radiat. Res.* **1965**, *26*, 483.
(90) Debye, P.; Hückel, E. *Phys. Z.* **1923**, *24*, 185.
(91) Davies, C. W. *Prog. React. Kinet.* **1961**, *1*, 161.
(92) Brönsted, J. N.; Livingston, R. *J. Am. Chem. Soc.* **1927**, *49*, 435.
(93) Davies, C. W. *Ion Association*; Butterworths: Washington, 1962.
(94) Iwata, A.; Yamanaka, C. *Anal. Chim. Acta* **1993**, *277*, 25.
(95) Schwarz, H. A.; Dodson, R. W. *J. Phys. Chem.* **1984**, *88*, 3643.
(96) Graedel, T. E.; Goldberg, K. I. *J. Geophys. Res.* **1983**, *88*, 10865.
(97) Steinfeld, J. I.; Francisco, J. S.; Hase, W. L. *Chemical Kinetics and Dynamics*, 2nd ed.; Prentice-Hall: Upper Saddle River, NJ, 1998.
(98) Huie, R. E. Free radical chemistry of the atmospheric aqueous phase. In *Progress and Problems in Atmospheric Chemistry*, 1st ed.; Barker, J. R., Ed.; World Scientific: Singapore, 1995; p 374.
(99) Lelieveld, J.; Crutzen, P. J. *Nature* **1990**, *343*, 227.
(100) Perner, D.; Arnold, T.; Crowley, J.; Klüpfel, T.; Martinez, M.; Seuwen, R. *J. Atmos. Chem.* **1999**, *34*, 9.
(101) Sander, R.; Crutzen, P. J. *J. Geophys. Res.* **1996**, *101*, 9121.
(102) Sumner, A. L.; Shepson, P. B. *Nature* **1999**, *398*, 230.
(103) Foster, K. L.; Plastridge, R. A.; Bottenheim, J. W.; Shepson, P. B.; Finlayson-Pitts, B. J.; Spicer, C. W. *Science* **2001**, *291*, 471.
(104) Finlayson-Pitts, B. J.; Hemminger, J. C. *J. Phys. Chem. A* **2000**, *104*, 11463.
(105) Kreyszig, E. Linear differential equations of second and higher order. In *Advanced Engineering Mathematics*, 8th ed.; Holland, B., Ed.; John Wiley & Sons: New York, 1999; Chapter 2, p 64.
(106) Ross, A. B.; Neta, P. *Rate Constants for Reactions of Inorganic Radicals in Aqeuous Solution*; U. S. Department of Commerce, 1979; Vol. 65.
(107) Christenen, H.; Sehested, K. *J. Phys. Chem.* **1988**, *92*, 3007.
(108) Elliot, A. J.; Buxton, G. V. *J. Chem. Soc., Faraday Trans.* **1992**, *88*, 2465.